

Foveal Blur-Boosted Segmentation of Nuclei in Histopathology Images with Shape Prior Knowledge and Probability Map Constraints

Hongyi Duanmu¹, Fusheng Wang^{1,2}, George Teodoro³, Jun Kong⁴

¹Department of Computer Science, Stony Brook University

¹Department of Biomedical Informatics, Stony Brook University

³Department of Computer Science, Federal University of Minas Gerais

⁴Department of Mathematics and Statistics, Georgia State University

Motivations & Challenges

- In pathology image analysis field, lack of training images is an obstacle for robust system constructing.
- In nuclei segmentation in pathology images, pathologists have prior knowledge in nuclei's common shapes, while CNN systems cannot explicitly be benefited from it.
- Main problem we attempt to solve is:
 - An easy and efficient method for enriching the dataset with limited sample size.
 - In terms of loss functions, design new terms in shape prior knowledge and morphological constraints.

Methods – Foveal Blur

Mimicking human's vision system, spatial frequency map is applied to the raw pathology images with focus on each single nucleus, enriching the dataset.

The input images is foveal blurred images with focus on each cell and the ground truth is only the mask of the corresponding nucleus.

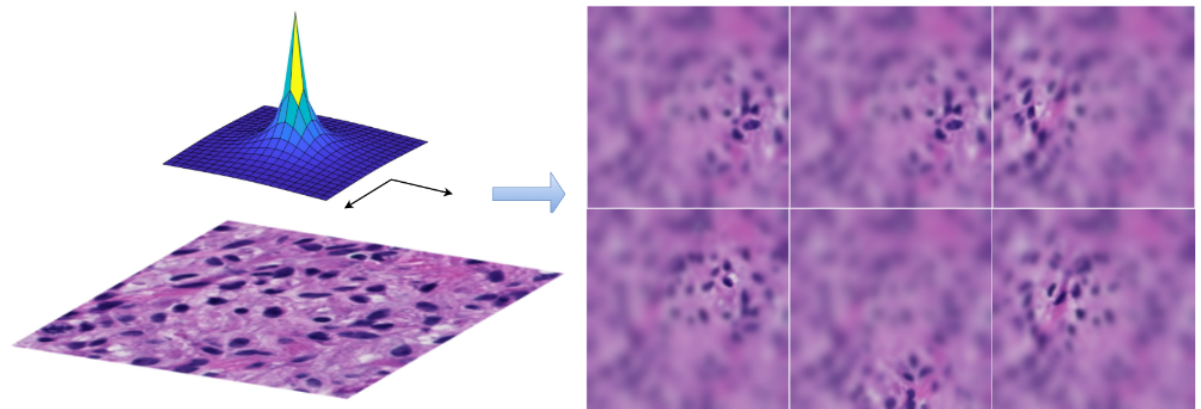


Fig. 1: We present an idealized spatial frequency map (top left), a raw histopathology image patch (bottom left), and multiple foveal blurred sample images (right) derived from the raw histopathology image patch.

Methods – Shape prior and smoothness

With a nuclei shape prior library built before, Shape Prior term (\mathcal{L}_{sp}) is designed to penalize nuclei contour predicted with wired shapes.

Smoothness term (\mathcal{L}_{sm}) was introduced to constrain the morphological smoothness with the first and second-order gradient of the predicted probability maps.

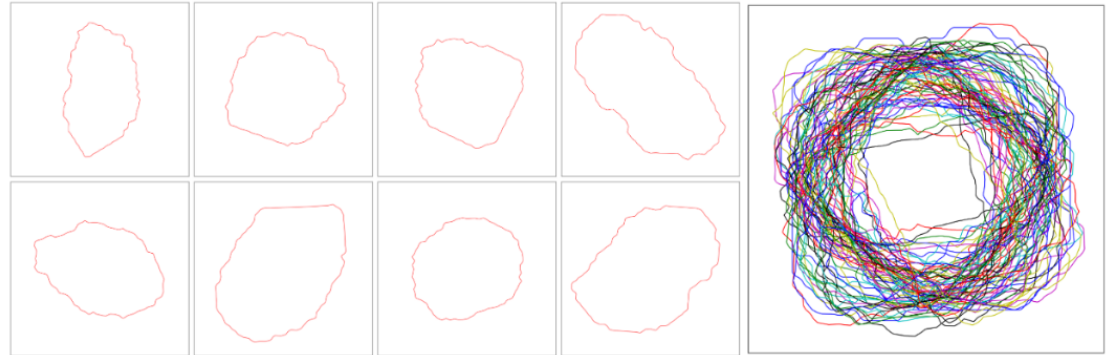


Fig. 2: Representative nuclei and the resulting nuclei shape prior library.

$$\mathcal{L}_{SP} = - \sum_{i=1}^N \max_k \int_{z \in \Omega} \Psi_k \otimes f(x_i(z)|\theta) dz$$

$$\mathcal{L}_{SM} = \sum_{i=1}^N \int_{z \in \Omega} (\|\nabla f(x_i(z)|\theta)\|_1 + \alpha \|\nabla^2 f(x_i(z)|\theta)\|_1) dz$$

Methods

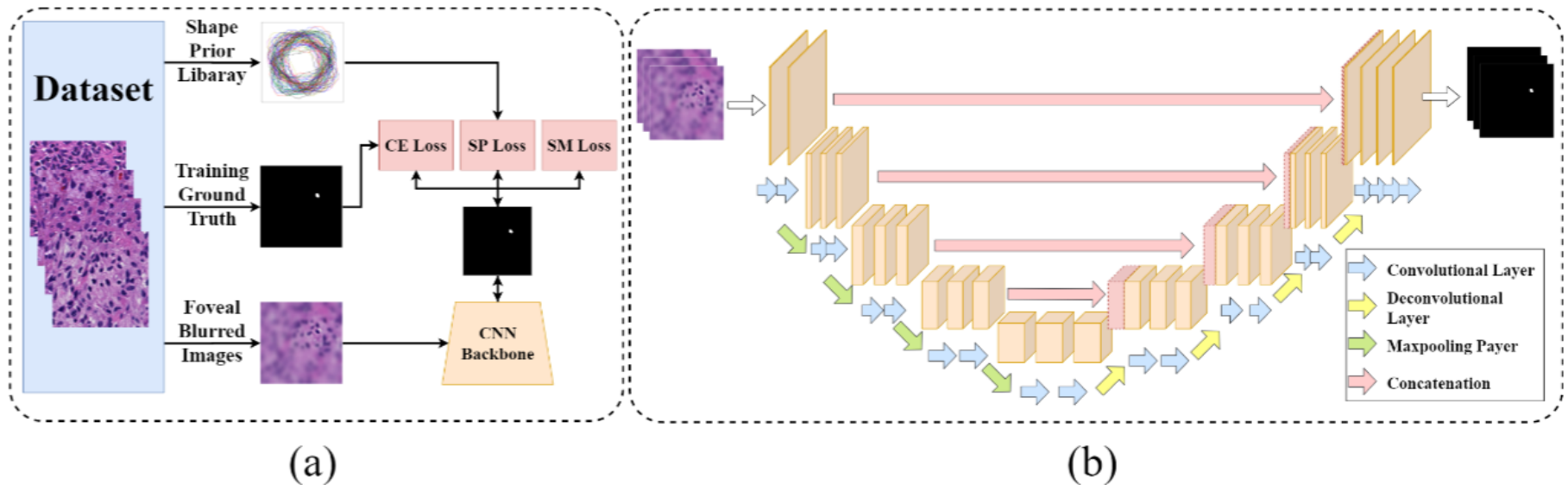


Fig. 3: We present the system schema with details of (a) the proposed system, and (b) CNN backbone architecture.

Dataset & Results

GBM: 40 H&E images with ~6,000 nuclei contours captured from Emory University Hospital.

TCGA: 36 H&E images with ~4,400 nuclei contours with all images and annotation public.

MoNuSeg: 44 H&E images with ~22,000 nuclei contoured from MICCAI'18 Challenge.

U-Net+DC: U-Net trained with Dice loss;

U-Net+CE: U-Net trained with cross entropy loss.

Table 1. Progressively improved results from our proposed systems are compared with the backbone U-Net model. The average Jaccard coefficient (J), Precision (P), Recall (R), Dice coefficient (DC), Accuracy (Acc), Panoptic Quality (PQ), and Hausdorff distance (HD) for three independent datasets are presented, respectively.

Metrics		U-Net+DC	U-Net+CE	FB-Net	FB+SP	FB+SP+SM
GBM	J (%)	68.70	70.96	75.36	77.92	80.02
	P (%)	83.76	82.90	87.04	90.32	91.75
	R (%)	83.48	83.16	84.91	85.11	86.27
	DC (%)	83.57	83.01	85.94	87.59	88.90
	Acc (%)	90.83	92.14	93.58	94.43	95.03
	PQ (%)	56.72	58.91	61.76	68.25	69.13
	HD (pixels)	41.07	41.12	39.47	39.02	37.21
TCGA	J (%)	72.60	72.26	76.78	78.28	81.80
	P (%)	86.81	83.23	86.50	87.13	91.32
	R (%)	85.07	84.30	87.10	88.52	88.90
	DC (%)	85.93	83.73	87.09	87.81	89.95
	Acc (%)	92.75	93.10	93.86	94.96	95.74
	PQ (%)	58.38	57.96	61.86	65.73	68.57
	HD (pixels)	49.56	49.02	48.37	46.72	44.98
MoNuSeg	J (%)	65.02	65.64	69.81	70.11	72.59
	P (%)	85.29	70.06	76.87	77.13	79.86
	R (%)	73.64	91.40	88.57	88.72	88.85
	DC (%)	78.71	79.21	82.17	82.38	84.03
	Acc (%)	90.34	89.63	91.66	91.77	92.66
	PQ (%)	47.35	50.43	55.48	54.01	60.84
	HD (pixels)	56.77	57.37	55.93	56.72	55.17

Results

Table 2. Performance comparison between state-of-the-art methods (both non-deep learning and deep learning models) and our proposed system (mean, std).

Metrics		mRLS	MOW	IVW	RACM	U-Net + CE	DLV3+	cGAN	Mask R-CNN	YOLCAT++	FB+SP+SM
GBM	J (%)	61.88 (4.88)	68.00 (2.27)	69.17 (1.79)	53.17 (3.05)	70.96 (1.88)	75.29 (1.93)	72.45 (1.35)	72.89 (1.91)	67.16 (5.54)	80.02 (0.97)
	P (%)	78.35 (2.00)	73.77 (1.88)	76.38 (2.03)	62.15 (2.11)	82.90 (2.17)	86.61 (1.70)	84.24 (1.37)	86.53 (0.69)	90.66 (1.10)	91.75 (2.17)
	R (%)	74.97 (7.89)	89.72 (3.28)	88.12 (3.65)	78.85 (6.35)	83.16 (1.91)	85.27 (3.36)	83.83 (1.65)	82.24 (2.32)	72.14 (6.06)	86.27 (1.88)
	DC (%)	76.35 (3.75)	80.93 (1.62)	81.76 (1.25)	69.38 (2.63)	83.01 (1.29)	85.89 (1.26)	84.02 (0.91)	84.31 (1.28)	80.22 (3.92)	88.90 (0.60)
	Acc (%)	86.47 (1.37)	90.15 (1.62)	90.32 (1.64)	84.47 (2.46)	92.14 (1.15)	93.53 (1.04)	92.63 (1.13)	92.65 (1.33)	91.62(2.35)	95.03 (0.70)
	PQ (%)	55.63 (1.86)	53.76 (2.34)	59.64 (2.66)	37.36 (4.24)	58.91 (2.53)	64.66 (1.89)	60.57 (2.07)	66.10 (1.79)	58.11 (7.33)	68.09 (1.57)
	HD (pixels)	47.58 (6.16)	40.48 (7.20)	39.05 (9.48)	42.69 (5.31)	41.12 (7.59)	39.39 (8.53)	40.91 (7.26)	39.53 (15.01)	37.45 (6.77)	37.21 (5.96)
TCGA	J (%)	56.08 (5.99)	74.31 (4.63)	72.86 (4.54)	57.44 (3.69)	72.26 (6.56)	76.68 (1.41)	74.65 (2.21)	81.84 (3.15)	61.44 (10.87)	81.80 (3.62)
	P (%)	86.15 (2.16)	87.66 (2.68)	89.00 (1.97)	73.92 (1.53)	83.23 (5.52)	87.33 (2.00)	92.92 (0.97)	91.50 (1.54)	97.37 (1.52)	91.32 (3.73)
	R (%)	61.67 (6.88)	83.08 (5.52)	80.07 (4.94)	72.22 (6.11)	84.30 (3.91)	86.31 (1.62)	81.42 (2.45)	88.58 (3.32)	62.22 (11.27)	88.90 (4.75)
	DC (%)	71.68 (5.00)	85.18 (3.11)	84.22 (3.09)	72.90 (3.01)	83.73 (4.53)	85.86 (2.35)	86.77 (1.41)	89.98 (1.93)	77.24 (9.69)	89.95 (2.21)
	Acc (%)	85.99 (1.96)	93.56 (2.02)	92.94 (2.18)	88.12 (2.16)	93.10 (2.17)	94.35 (0.83)	95.03 (0.58)	95.81 (1.10)	80.31 (6.73)	95.74 (1.13)
	PQ (%)	53.11 (6.07)	56.37 (1.35)	60.05 (2.92)	45.18 (0.94)	57.96 (2.10)	64.60 (1.93)	63.60 (2.01)	68.09 (2.80)	56.06 (8.51)	69.91 (2.16)
	HD (pixels)	54.66 (16.72)	48.54 (4.12)	46.11 (8.38)	45.08 (8.26)	49.02 (9.10)	47.88 (8.69)	48.72 (10.17)	47.48 (20.14)	65.87 (21.77)	44.98 (10.44)
MoNuSeg	J (%)	53.40 (4.37)	55.57 (13.41)	67.77 (5.60)	44.27 (8.68)	65.64 (3.44)	69.38 (3.81)	67.99 (3.32)	66.24 (6.32)	51.24 (4.97)	72.59 (5.14)
	P (%)	87.61 (4.43)	92.39 (4.81)	90.80 (3.24)	75.09 (3.92)	70.06 (3.95)	76.08 (4.43)	73.96 (3.69)	78.25 (9.29)	68.92 (6.97)	79.86 (5.05)
	R (%)	57.83 (5.09)	58.95 (16.17)	72.70 (5.15)	52.35 (12.81)	91.40 (3.86)	88.94 (4.38)	89.57 (4.28)	81.99 (5.64)	67.05 (6.46)	88.85 (3.62)
	DC (%)	69.55 (3.70)	70.80 (11.14)	80.70 (4.06)	61.04 (8.21)	79.21 (2.54)	81.86 (2.63)	80.91 (2.39)	79.51 (4.72)	67.62 (4.44)	84.03 (3.39)
	Acc (%)	83.32 (1.53)	82.50 (9.44)	90.55 (1.86)	78.81 (5.58)	89.63 (1.05)	91.46 (1.34)	90.86 (1.01)	91.56 (2.70)	85.28 (0.83)	92.66 (1.65)
	PQ (%)	49.55 (1.54)	34.68 (13.82)	51.00 (8.89)	30.78 (4.42)	50.43 (2.60)	57.30 (2.35)	53.58 (2.63)	60.33 (6.98)	54.17 (8.40)	60.84 (3.47)
	HD (pixels)	68.86 (11.96)	57.47 (7.39)	56.54 (6.61)	56.31 (8.47)	57.37 (6.63)	55.86 (7.52)	56.38 (7.15)	55.76 (15.22)	66.99 (9.92)	55.17 (7.07)

Limits & Future Work

- Quantify the system's sensitivity to the parameters of foveal blur and explore more the mechanism of foveal blur.
- The shape prior library is static and it would be better to embed the library building into the system to make it dynamic in the training.
- As there are three components in the loss function, it should be explored more on the hyperparameters to balance those three.